Research Square

Preprints are preliminary reports that have not undergone peer review.
They should not be considered conclusive, used to inform clinical practice,
or referenced by the media as validated information.

Energy Preserving Parametric Multi-symplectic Methods for the Gross-Pitaevskii Equation

Rong Gao
Jiangxi Flight University
Linghua Kong
konglh@mail.ustc.edu.cn
Jiangxi Normal University
Futuan Li
Beijing Normal-Hong Kong Baptist University

Research Article

Keywords:

Posted Date: November 2nd, 2026

DOI: https://doi.org/10.21203/rs.3.rs-11093804/v1

License: This work is licensed under a Creative Commons Attribution 4.0 International License.
Read Full License

Additional Declarations: No competing interests reported.

Energy Preserving Parametric Multi-symplectic Methods for the Gross-Pitaevskii Equation

Rong Gao · Linghua Kong⋆ · Futuan Li

Received: date / Accepted: date

Abstract The multi-symplectic structure and energy conservation are inherent properties of the Gross-Pitaevskii equation. In this paper, we propose classical multi-symplectic Runge-Kutta methods and parametric multi-symplectic Runge-Kutta methods for the one-dimensional Gross-Pitaevskii equation. The parametric methods not only inherit the multi-symplectic structure and quadratic invariants of the classical methods, but also achieve energy conservation in a weaker sense by introducing an additional parameter. Numerical experiments verify the effectiveness of the proposed methods.

Keywords Gross-Pitaevskii equations · Multi-symplectic methods · Parametric multi-symplectic methods · Energy conservation.

Mathematics Subject Classification (2020) 65M06 · 65M12 · 65Z05 · 70H15

1 Introduction

The Gross-Pitaevskii equation (GPE), independently derived by Gross and Pitaevskii [1,2] in 1961, is a nonlinear Schrödinger-type equation tailored to describe the evolution of wave functions in condensed matter systems, especially in Bose-Einstein condensation (BEC) [3–7]. It considers particle interactions and effectively captures the dynamical behavior and stability of the condensate. By solving the GPE, one can obtain the ground state and excited states of the condensate, facilitating an analysis of its physical properties. In this paper, we consider the following GPE in dimensionless form [8]

$$\mathrm{i}\partial_t u = \left(-\frac{1}{2}\Delta + \theta(\mathbf{x}) + \beta|u|^2\right)u, \quad \mathbf{x} \in \mathbb{R}^d, \quad t > 0, \tag{1.1}$$

where $u(\mathbf{x}, t)$ denotes the macroscopic wave function of the condensate, with the initial condition $u(\mathbf{x}, 0) = u_0$. The potential $\theta(\mathbf{x})$ is a real-valued function, typically generated experimentally. The parameter β represents the strength of the interatomic interaction.

⋆ Corresponding author: E-mail: konglh@mail.ustc.edu.cn

Gaorong
1. School of Aviation Mechatronics Engineering, Jiangxi Flight University,
Nanchang, Jiangxi, 330088, China
2. School of Mathematics and Statistics, Jiangxi Normal University, Nanchang, Jiangxi, 330022, P. R. China

Linghua Kong
2. School of Mathematics and Statistics, Jiangxi Normal University, Nanchang, Jiangxi, 330022, P. R. China

Futuan Li
3. Faculty of Science and Technology, Beijing Normal-Hong Kong Baptist University,
Zhuhai, Guangdong 519087, China

Taking the inner product of equation (1.1) with $u(\mathbf{x},t)$ and extracting the imaginary part yields the mass conservation law

$$\mathcal{M}(t)=\int_{\mathbb{R}^d}|u(\mathbf{x},t)|^2\,\mathrm{d}\mathbf{x}\equiv\mathcal{M}(0).$$

Taking the inner product of equation (1.1) with the time derivative $\partial_t u(\mathbf{x},t)$ and extracting the real part results in the energy conservation law

$$\mathcal{H}(t)=\int_{\mathbb{R}^d}\left[\frac{1}{2}|\nabla u|^2+\theta(\mathbf{x})|u|^2+\frac{\beta}{2}|u|^4\right]\mathrm{d}\mathbf{x}\equiv\mathcal{H}(0).$$

The GPE admits several conserved quantities, including mass, energy, symplecticity, and multi-symplecticity, corresponding to the preservation of physical properties and geometric structures, respectively. For general Hamiltonian PDEs, it is generally impossible for a constant time-stepping numerical method to simultaneously preserve both geometric structures and physical properties [9,10]. Classical symplectic methods preserve quadratic invariants exactly, but fail to preserve non-quadratic Hamiltonian functionals. Inspired by the energy and quadratic invariant preserving (EQUIP) method proposed by Brugnano et al. [11] and Chen et al. [12], this paper constructs multi-symplectic Runge-Kutta (RK) methods and parametric multi-symplectic RK methods for the numerical simulation of the aforementioned equation. The parametric methods not only preserve the multi-symplectic geometric structure, but also satisfy the mass and energy conservation laws.

A numerical method that preserves the discrete multi-symplectic conservation law is referred to as a multi-symplectic method for Hamiltonian systems [13,14]. Over the past two decades, such methods have attracted considerable attention [15–18]. For example, Tian et al. [19] developed a multi-symplectic difference scheme for the two-dimensional GPE with rotating angular momentum. Kong et al. [20,21] proposed high-order compact splitting multi-symplectic schemes for the single-component GPE without vortex and angular momentum terms. Wang et al. [22] proposed a multi-symplectic scheme for the coupled GPE with angular momentum rotating terms. The strategy of achieving energy conservation by introducing a tunable parameter at each step was first proposed by [23] and subsequently developed by [11,24,25] into the EQUIP framework. Building on this, Chen et al. [12] extended the framework from ODEs to PDEs, demonstrating its application through the numerical solution of the Hamiltonian wave equation. Sim et al. [26] extended the original EQUIP method to the GEQUIP method. By introducing additional parameters, the scheme preserves the symplectic structure while exactly conserving multiple physical invariants of Hamiltonian systems, not only energy. In contrast, Cai and Wang [27] introduced the scalar auxiliary variable (SAV) approach to construct two classes of linearly implicit energy-preserving schemes for general multi-symplectic Hamiltonian PDEs. This paper adopts the EQUIP multi-symplectic method, which extends the classical multi-symplectic Runge-Kutta scheme by introducing a real parameter α. At each grid cell defined by the spatial step h and the time step τ, α is determined by simultaneously solving the modified multi-symplectic RK discretization alongside the local energy conservation equation. Unlike strictly conservative methods, the EQUIP approach exhibits weak energy conservation, with the existence and value of α depending on both the step sizes and the initial conditions.

The rest of the paper is organized as follows. In Section 2, we transform the one-dimensional GPE into a multi-symplectic Hamiltonian system, present its multi-symplectic structure and conservation laws, and construct fully discrete multi-symplectic RK schemes. In Section 3, we formulate parametric multi-symplectic RK methods and analyze the existence and uniqueness of the parameter. In Section 4, we provide numerical examples for both the multi-symplectic RK methods and the parametric multi-symplectic RK methods to validate the theoretical analysis and numerical performance. Section 5 concludes the paper.

2 Multi-symplectic Runge-Kutta methods

In this section, the one-dimensional GPE is transformed into a classical multi-symplectic Hamiltonian system, and multi-symplectic RK methods are constructed.

2.1 Multi-symplectic structure

To simplify the computation, this paper considers the one-dimensional case with periodic boundary conditions. Let $u = p + \mathrm{i}q$, and denote its spatial derivative by $\partial_x u = \partial_x p + \mathrm{i}\partial_x q \triangleq v + \mathrm{i}w$. The GPE (1.1) can then be rewritten as the following system of first-order differential equations:

$$\begin{cases} -2\,q_t + v_x = 2\,p\left[\theta(x) + \beta\left(p^2+q^2\right)\right], \\ 2\,p_t + w_x = 2\,q\left[\theta(x) + \beta\left(p^2+q^2\right)\right], \\ p_x = v, \\ q_x = w, \end{cases}$$

where $p = p(x,t)$ and $q = q(x,t)$ are real-valued functions, and $\mathrm{i} = \sqrt{-1}$ denotes the imaginary unit. Accordingly, this system can be recast as a classical multi-symplectic Hamiltonian system

$$M\,\partial_t z + K\,\partial_x z = \nabla_z S(z), \qquad (x,t) \in \mathbb{R} \times \mathbb{R}_+, \tag{2.1}$$

where $z = (p, q, v, w)^{\mathrm{T}}$, and the Hamiltonian functional is

$$S(z) = -\frac{1}{2}(v^2+w^2) + \theta(x)(p^2+q^2) + \frac{\beta}{2}(p^2+q^2)^2,$$

The skew-symmetric matrices M and K are defined as follows:

$$M = \begin{bmatrix} 0 & -2 & 0 & 0 \\ 2 & 0 & 0 & 0 \\ 0 & 0 & 0 & 0 \\ 0 & 0 & 0 & 0 \end{bmatrix}, \qquad K = \begin{bmatrix} 0 & 0 & 1 & 0 \\ 0 & 0 & 0 & 1 \\ -1 & 0 & 0 & 0 \\ 0 & -1 & 0 & 0 \end{bmatrix}.$$

For the Hamiltonian system (2.1), the multi-symplectic structure and conservation laws are two of its core properties. The multi-symplectic structure can be expressed as

$$\partial_t\,\omega + \partial_x\,\kappa = 0, \tag{2.2}$$

where $\omega = \mathrm{d}z \wedge M\,\mathrm{d}z = -4\,\mathrm{d}p \wedge \mathrm{d}q$, and $\kappa = \mathrm{d}z \wedge K\,\mathrm{d}z = 2(\mathrm{d}p \wedge \mathrm{d}v + \mathrm{d}q \wedge \mathrm{d}w)$. The conservation laws include the energy conservation law (ECL) and the momentum conservation law (MCL). Specifically, the local ECL can be expressed as:

$$\partial_t E(z) + \partial_x F(z) = 0, \tag{2.3}$$

where the energy density $E(z)$ and the energy flux $F(z)$ are given by

$$\begin{aligned} E(z) &= S(z) - \frac{1}{2}z^{\mathrm{T}}K\partial_x z = \frac{1}{2}(v^2+w^2) + \theta(x)(p^2+q^2) + \frac{\beta}{2}(p^2+q^2)^2, \\ F(z) &= \frac{1}{2}z^{\mathrm{T}}K\partial_t z = -(v\,\partial_t p + w\,\partial_t q); \end{aligned}$$

while the local MCL can be written as:

$$\partial_t I(z) + \partial_x G(z) = 0, \tag{2.4}$$

where the momentum density $I(z)$ and the momentum flux $G(z)$ are given by

$$\begin{aligned} I(z) &= \frac{1}{2}z^{\mathrm{T}}M\partial_x z = -pw + qv, \\ G(z) &= S(z) - \frac{1}{2}z^{\mathrm{T}}M\partial_t z = S(z) + (p\,\partial_t q - q\,\partial_t p). \end{aligned}$$

Remark 2.1 *Under the periodic boundary condition $u(0,t) = u(L,t)$, the local energy conservation law directly implies global energy conservation. Defining the global energy as $\mathcal{H}(t) := \int_0^L E(z)\,\mathrm{d}x$ and integrating the local conservation law (2.3) over $[0,L]$ yields*

$$\frac{\mathrm{d}\mathcal{H}(t)}{\mathrm{d}t} = 0,$$

which establishes global energy conservation. This derivation applies equally to other locally conserved quantities, such as momentum.

2.2 Multi-symplectic RK schemes

Hong et al. [13] showed that applying symplectic RK schemes in both space and time preserves the multi-symplecticity of general Hamiltonian PDEs. First, the space-time plane is uniformly partitioned with spatial step size h and temporal step size τ, and the mesh function of $u(x,t)$ is denoted by $\{u_{j,k} \mid (x_j,t_k) \in \mathbb{R}\times\mathbb{R}_+\}$. For theoretical analysis, the discussion is restricted to a single grid cell $[x_0,x_1]\times[t_0,t_1]$.

Then, an s-stage symplectic RK scheme (c,A,b) and an r-stage symplectic RK scheme $(\tilde{c},\tilde{A},\tilde{b})$ are applied to the spatial and temporal discretization of the multi-symplectic form (2.1) of the GPE (1.1), respectively . We obtain a fully discrete scheme:

$$
\begin{aligned}
&P_{i,m} = p_0^{[m]} + h\sum_{j=1}^{s} a_{ij}\partial_x P_{j,m}, \qquad v_1^{[m]} = v_0^{[m]} + h\sum_{i=1}^{s} b_i\partial_x V_{i,m},\\
&Q_{i,m} = q_0^{[m]} + h\sum_{j=1}^{s} a_{ij}\partial_x Q_{j,m}, \qquad w_1^{[m]} = w_0^{[m]} + h\sum_{i=1}^{s} b_i\partial_x W_{i,m},\\
&p_1^{[m]} = p_0^{[m]} + h\sum_{i=1}^{s} b_i\partial_x P_{i,m}, \qquad P_{i,m} = p_{[i]}^{0} + \tau\sum_{n=1}^{r} \tilde{a}_{mn}\partial_t P_{i,n},\\
&q_1^{[m]} = q_0^{[m]} + h\sum_{i=1}^{s} b_i\partial_x Q_{i,m}, \qquad Q_{i,m} = q_{[i]}^{0} + \tau\sum_{n=1}^{r} \tilde{a}_{mn}\partial_t Q_{i,n},\\
&V_{i,m} = v_0^{[m]} + h\sum_{j=1}^{s} a_{ij}\partial_x V_{j,m}, \qquad p_{[i]}^{1} = p_{[i]}^{0} + \tau\sum_{m=1}^{r} \tilde{b}_m\partial_t P_{i,m},\\
&W_{i,m} = w_0^{[m]} + h\sum_{j=1}^{s} a_{ij}\partial_x W_{j,m}, \qquad q_{[i]}^{1} = q_{[i]}^{0} + \tau\sum_{m=1}^{r} \tilde{b}_m\partial_t Q_{i,m},\\
&\partial_x P_{i,m} = V_{i,m}, \quad \partial_x Q_{i,m} = W_{i,m},\\
&\partial_t P_{i,m} + \frac{1}{2}\partial_x W_{i,m} = \left[\theta(c_i h) + \beta(P_{i,m}^2 + Q_{i,m}^2)\right] Q_{i,m},\\
&-\partial_t Q_{i,m} + \frac{1}{2}\partial_x V_{i,m} = \left[\theta(c_i h) + \beta(P_{i,m}^2 + Q_{i,m}^2)\right] P_{i,m},
\end{aligned}
\tag{2.5}
$$

where $A = (a_{ij})_{i,j=1}^{s}$ and $\tilde{A} = (\tilde{a}_{mn})_{m,n=1}^{r}$ are coefficient matrices, $b = (b_1,\cdots,b_s)^{\mathrm{T}}$ and $\tilde{b} = (\tilde{b}_1,\cdots,\tilde{b}_r)^{\mathrm{T}}$ are weight vectors, and the abscissae are

$$
c_i = \sum_{j=1}^{s} a_{ij}, \quad i = 1,\cdots,s; \;\; d_m = \sum_{n=1}^{r} \tilde{a}_{mn}, \quad m = 1,\cdots,r.
$$

We denote $P_{i,m} \approx p(c_i h, d_m\tau)$ for the numerical values at the RK stage points, and $p_1^{[m]} \approx p(h, d_m\tau)$, $p_{[i]}^{1} \approx p(c_i h,\tau)$ for those at the cell boundaries.

The scheme (2.5) preserves the multi-symplecticity provided that

$$
\begin{cases}
M \equiv BA + A^{\mathrm{T}}B - bb^{\mathrm{T}} = 0,\\
\tilde{M} \equiv \tilde{B}\tilde{A} + \tilde{A}^{\mathrm{T}}\tilde{B} - \tilde{b}\tilde{b}^{\mathrm{T}} = 0,
\end{cases}
\tag{2.6}
$$

where $B = \mathrm{diag}(b)$ and $\tilde{B} = \mathrm{diag}(\tilde{b})$ are diagonal matrices with diagonal entries b_i and $\tilde{b}_m$, respectively.

Example 2.1 Let $r = 1$ and $s = 2$. The Butcher tableaux of the symplectic RK schemes in the spatial and temporal directions are respectively given by

$$
\begin{array}{c|c} \frac{1}{2} & \frac{1}{2} \\ \hline & 1 \end{array}
\qquad
\begin{array}{c|cc}
\frac{1}{2}-\frac{\sqrt{3}}{6} & \frac{1}{4} & \frac{1}{4}-\frac{\sqrt{3}}{6} \\
\frac{1}{2}+\frac{\sqrt{3}}{6} & \frac{1}{4}+\frac{\sqrt{3}}{6} & \frac{1}{4} \\ \hline
 & \frac{1}{2} & \frac{1}{2}
\end{array}
$$

In this case, the spatial direction uses a fourth-order Gauss collocation method, the temporal direction uses the midpoint rule, and both satisfy the multi-symplectic conditions (2.6), thereby yielding a multi-symplectic Gauss collocation method.

The discrete energy conservation law corresponding to (2.3) is

$$\sum_{i=1}^{s} b_i \left(E_i^1 - E_i^0\right) h + \sum_{m=1}^{r} \tilde{b}_m \left(F_1^m - F_0^m\right) \tau = 0, \tag{2.7}$$

here

$$E_i^l = \frac{1}{2}\left[(v_{[i]}^l)^2 + (w_{[i]}^l)^2\right] + \theta(c_i h)\left[(p_{[i]}^l)^2 + (q_{[i]}^l)^2\right] + \frac{\beta}{2}\left[(p_{[i]}^l)^2 + (q_{[i]}^l)^2\right]^2, \tag{2.8}$$

$$F_l^m = -\left[v_l^{[m]}(\partial_t p)_l^{[m]} + w_l^{[m]}(\partial_t q)_l^{[m]}\right], \quad l = 0, 1. \tag{2.9}$$

and the discrete MCL can be formulated analogously. Unfortunately, the scheme (2.5) fails to satisfy discrete energy conservation law (2.7). To this end, we insert a parameter α into to scheme (2.5) to enforce local energy conservation (2.7), leading to parametric multi-symplectic RK schemes.

3 Parametric multi-symplectic Runge-Kutta methods

In this section, we introduce a real parameter into the multi-symplectic Gauss collocation method to construct a parametric discrete scheme that preserves the multi-symplectic structure. By further incorporating the discrete ECL into the system, we prove the existence and uniqueness of both the numerical solution and the parameter.

3.1 Parametric multi-symplectic RK schemes

Let (c, A, b) be an s-stage Gauss RK method. The shifted normalized Legendre polynomials on $[0, 1]$ are defined as

$$P_k(x) = \frac{\sqrt{2k+1}}{k!}\frac{\mathrm{d}^k}{\mathrm{d}x^k}(x^k(x-1)^k),$$

of which the lowest-degree examples are

$$P_0(x) = 1, \quad P_1(x) = \sqrt{3}(2x-1), \quad P_2(x) = \sqrt{5}(6x^2 - 6x + 1).$$

Define the generalized Vandermonde matrix $W = (w_{ij})_{i,j=1}^s$ by

$$w_{ij} = P_{j-1}(c_i), \quad i, j = 1, 2, \cdots, s.$$

Then, under this transformation, the coefficient matrix A of the s-stage Gauss method is reduced to the tridiagonal form [28]:

$$X = W^{-1}AW = \begin{pmatrix} \frac{1}{2} & -\xi_1 & & & \\ \xi_1 & 0 & -\xi_2 & & \\ & \xi_2 & \ddots & \ddots & \\ & & \ddots & 0 & -\xi_{s-1} \\ & & & \xi_{s-1} & 0 \end{pmatrix},$$

with $\xi_k = \frac{1}{2\sqrt{4k^2-1}}$. Following the idea of EQUIP methods introduced in [11,25,12], we define the perturbation matrices $X(\alpha)$ as

$$X(\alpha) = X + \alpha V, \tag{3.1}$$

where α is a real parameter and V is the skew?symmetric matrix

$$V = \begin{pmatrix} 0 & 0 & & & & \\ 0 & \ddots & \ddots & & & \\ & \ddots & \ddots & -1 & & \\ & & 1 & \ddots & \ddots & \\ & & & \ddots & \ddots & 0 \\ & & & & 0 & 0 \end{pmatrix}.$$

Let the multi-symplectic RK scheme (2.5) employ the s-stage and r-stage Gauss RK methods (c, A, b) and $(\tilde{c}, \tilde{A}, \tilde{b})$ for the spatial and temporal discretizations, respectively. We now define the parametric multi?symplectic RK schemes $(c, A(\alpha), b)$ and $(\tilde{c}, \tilde{A}(\alpha), \tilde{b})$.

Definition 3.1 *The parametric multi-symplectic RK scheme is obtained by replacing the coefficient matrices with*

$$A(\alpha) = WX(\alpha)W^{-1} = A + \alpha WVW^{-1}, \tag{3.2}$$

$$\tilde{A}(\alpha) = \tilde{W}\tilde{X}(\alpha)\tilde{W}^{-1} = \tilde{A} + \alpha\tilde{W}\tilde{V}\tilde{W}^{-1}. \tag{3.3}$$

where W, V and $\tilde{W}$, $\tilde{V}$ are the generalized Vandermonde matrices and the skew-symmetric matrices corresponding to the spatial and temporal directions, respectively, with $X(\alpha) = X + \alpha V$ and $\tilde{X}(\alpha) = \tilde{X} + \alpha\tilde{V}$.

Theorem 3.1 *For any real parameter α, the corresponding parametric method in* (3.2)-(3.3) *is also multi-symplectic.*

Proof: Since (c, b) are the nodes and weights of the s-point Gauss-Legendre quadrature on $[0, 1]$ and the degree of $P_{i-1}(x)P_{j-1}(x)$ is at most $2s - 2$, the quadrature formula is exact, yielding

$$\int_0^1 P_{i-1}(x)P_{j-1}(x)\,\mathrm{d}x = \sum_{k=1}^{s} b_k P_{i-1}(c_k)P_{j-1}(c_k) = \delta_{ij}, \quad i, j = 1, \cdots, s,$$

where δ_{ij} is the Kronecker delta. In matrix form, this reads

$$W^{\mathrm{T}}BW = I_s,$$

with I_s being the $s \times s$ identity matrix. The original method is multi-symplectic and V is skew-symmetric, so

$$\begin{aligned}
&BA(\alpha) + A(\alpha)^{\mathrm{T}}B - bb^{\mathrm{T}} \\
=&BA + A^{\mathrm{T}}B - bb^{\mathrm{T}} + \alpha BWVW^{-1} + \alpha(W^{-1})^{\mathrm{T}}V^{\mathrm{T}}W^{\mathrm{T}}B \\
=&\alpha(W^{\mathrm{T}})^{-1}(V + V^{\mathrm{T}})W^{-1} \\
=&0.
\end{aligned}$$

By the same reason, $\tilde{B}\tilde{A}(\alpha) + \tilde{A}(\alpha)^{\mathrm{T}}\tilde{B} - \tilde{b}\tilde{b}^{\mathrm{T}} = 0$. □

For $\alpha = 0$, the parametric multi?symplectic Runge-Kutta schemes $(c, A(\alpha), b)$ and $(\tilde{c}, \tilde{A}(\alpha), \tilde{b})$ reduce to the standard multi?symplectic Gauss collocation method. Although Definition 3.1 introduces α in both the spatial and temporal discretizations, in practice it suffices to perturb only one of them. An explicit example is given below.

Example 3.1 We derive the coefficient matrix of the parametric multi?symplectic RK method with $s = 2$, $r = 1$. The time discretization is the one?stage Gauss method, which requires no parameter. In space, $s = 2$. The generalized Vandermonde matrix and its inverse are

$$W = \begin{pmatrix} P_0(c_1) & P_1(c_1) \\ P_0(c_2) & P_1(c_2) \end{pmatrix} = \begin{pmatrix} 1 & -1 \\ 1 & 1 \end{pmatrix}, \quad W^{-1} = \frac{1}{2}\begin{pmatrix} 1 & 1 \\ -1 & 1 \end{pmatrix},$$

with $c_1 = \frac{1}{2} - \frac{\sqrt{3}}{6}$, $c_2 = \frac{1}{2} + \frac{\sqrt{3}}{6}$. Taking the skew-symmetric perturbation matrix

$$V = \begin{pmatrix} 0 & -1 \\ 1 & 0 \end{pmatrix},$$

a direct calculation gives $WVW^{-1} = V$. Hence the parametric coefficient matrix in space is $A(\alpha) = A + \alpha V$. The $s = 2$, $r = 1$ method is then by the two Butcher tableaux

$$\begin{array}{c|c} \frac{1}{2} & \frac{1}{2} \\ \hline & 1 \end{array} \qquad \begin{array}{c|cc} \frac{1}{2} - \frac{\sqrt{3}}{6} & \frac{1}{4} & \frac{1}{4} - \frac{\sqrt{3}}{6} - \alpha \\ \frac{1}{2} + \frac{\sqrt{3}}{6} & \frac{1}{4} + \frac{\sqrt{3}}{6} + \alpha & \frac{1}{4} \\ \hline & \frac{1}{2} & \frac{1}{2} \end{array}$$

For $\alpha = 0$, the space scheme reduces to the classical fourth?order Gauss method.

3.2 Existence and uniqueness of the parameter

Combining the parametric multi-symplectic RK scheme (3.2)-(3.3) with the discrete ECL (2.7) yields a nonlinear system of $8rs+1$ unknowns:

$$\begin{cases} P_{i,m} = p_0^{[m]} + h\sum_{j=1}^{s} a_{ij}(\alpha)V_{j,m}, \quad Q_{i,m} = q_0^{[m]} + h\sum_{j=1}^{s} a_{ij}(\alpha)W_{j,m}, \\ V_{i,m} = v_0^{[m]} + h\sum_{j=1}^{s} a_{ij}(\alpha)\partial_x V_{j,m}, \quad W_{i,m} = w_0^{[m]} + h\sum_{j=1}^{s} a_{ij}(\alpha)\partial_x W_{j,m}, \\ P_{i,m} = p_{[i]}^0 + \tau\sum_{n=1}^{r} \tilde{a}_{mn}(\alpha)\partial_t P_{i,n}, \quad Q_{i,m} = q_{[i]}^0 + \tau\sum_{n=1}^{r} \tilde{a}_{mn}(\alpha)\partial_t Q_{i,n}, \\ \partial_t P_{i,m} + \frac{1}{2}\partial_x W_{i,m} = \left[\theta(c_i h) + \beta(P_{i,m}^2 + Q_{i,m}^2)\right] Q_{i,m}, \\ -\partial_t Q_{i,m} + \frac{1}{2}\partial_x V_{i,m} = \left[\theta(c_i h) + \beta(P_{i,m}^2 + Q_{i,m}^2)\right] P_{i,m}, \\ h\sum_{i=1}^{s} b_i\left(E_i^1 - E_i^0\right) + \tau\sum_{m=1}^{r} \tilde{b}_m\left(F_1^m - F_0^m\right) = 0. \end{cases} \tag{3.4}$$

Define

$$\begin{aligned} P &= (P_1, P_2, \cdots, P_r)^{\mathrm{T}}, & \partial_t P &= (\partial_t P_1, \partial_t P_2, \cdots, \partial_t P_r)^{\mathrm{T}}, \\ Q &= (Q_1, Q_2, \cdots, Q_r)^{\mathrm{T}}, & \partial_t Q &= (\partial_t Q_1, \partial_t Q_2, \cdots, \partial_t Q_r)^{\mathrm{T}}, \\ V &= (V_1, V_2, \cdots, V_r)^{\mathrm{T}}, & \partial_x V &= (\partial_x V_1, \partial_x V_2, \cdots, \partial_x V_r)^{\mathrm{T}}, \\ W &= (W_1, W_2, \cdots, W_r)^{\mathrm{T}}, & \partial_x W &= (\partial_x W_1, \partial_x W_2, \cdots, \partial_x W_r)^{\mathrm{T}}, \end{aligned}$$

where $P_m = (P_{1,m}, P_{2,m}, \cdots, P_{s,m}) \in \mathbb{R}^s$ and the remaining vectors Q_m, V_m, W_m, $\partial_t P_m$, $\partial_t Q_m$, $\partial_x V_m$, $\partial_x W_m$ are defined analogously. We further set

$$\begin{aligned} p_0 &= (p_0^{[1]}, p_0^{[2]}, \cdots, p_0^{[r]})^{\mathrm{T}}, & p_1 &= (p_1^{[1]}, p_1^{[2]}, \cdots, p_1^{[r]})^{\mathrm{T}}, \\ p^0 &= (p_{[1]}^0, p_{[2]}^0, \cdots, p_{[s]}^0)^{\mathrm{T}}, & p^1 &= (p_{[1]}^1, p_{[2]}^1, \cdots, p_{[s]}^1)^{\mathrm{T}}, \\ F_0 &= (F_0^1, F_0^2, \cdots, F_0^r)^{\mathrm{T}}, & F_1 &= (F_1^1, F_1^2, \cdots, F_1^r)^{\mathrm{T}}, \\ E^0 &= (E_1^0, E_2^0, \cdots, E_s^0)^{\mathrm{T}}, & E^1 &= (E_1^1, E_2^1, \cdots, E_s^1)^{\mathrm{T}}, \end{aligned}$$

and define similarly q_0, q_1, q^0, q^1, v_0, v_1, v^0, v^1, w_0, w_1, w^0, w^1, $(\partial_t p)_0, (\partial_t p)_1, (\partial_t q)_0, (\partial_t q)_1$. In these notations, the nonlinear system (3.4) takes the compact form

$$\begin{cases} P = p_0 \otimes e_s + h\left[I_r \otimes A(\alpha)\right] V, \quad Q = q_0 \otimes e_s + h\left[I_r \otimes A(\alpha)\right] W, \\ V = v_0 \otimes e_s + h\left[I_r \otimes A(\alpha)\right] \partial_x V, \ W = w_0 \otimes e_s + h\left[I_r \otimes A(\alpha)\right] \partial_x W, \\ P = e_r \otimes p^0 + \tau[\tilde{A}(\alpha) \otimes I_s]\partial_t P, \quad Q = e_r \otimes q^0 + \tau[\tilde{A}(\alpha) \otimes I_s]\partial_t Q, \\ \partial_t P + \frac{1}{2}\partial_x W = \left[e_r \otimes \theta(ch) + \beta(P^2 + Q^2)\right] Q, \\ -\partial_t Q + \frac{1}{2}\partial_x V = \left[e_r \otimes \theta(ch) + \beta(P^2 + Q^2)\right] P, \\ b^T\left(E^1 - E^0\right) h + \tilde{b}^T\left(F_1 - F_0\right)\tau = 0, \end{cases} \tag{3.5}$$

where $\otimes$ denotes the Kronecker product, $e_s = (1, 1, \cdots, 1)^{\mathrm{T}} \in \mathbb{R}^s$, $e_r = (1, 1, \cdots, 1)^{\mathrm{T}} \in \mathbb{R}^r$, $A(\alpha) = (a_{ij}(\alpha))_{i,j=1}^s$, $\tilde{A}(\alpha) = (\tilde{a}_{mn}(\alpha))_{m,n=1}^r$, and $\theta(ch) = (\theta(c_1 h), \theta(c_2 h), \cdots, \theta(c_s h))^{\mathrm{T}}$.

By the definitions of E_i^l and F_l^m in (2.8) and (2.9), the last equation of (3.5) reduces to a form involving only the boundary vectors v_0, w_0, $(\partial_t p)_0$, $(\partial_t q)_0$, p^0, q^0, v^0, w^0 and v_1, w_1, $(\partial_t p)_1$, $(\partial_t q)_1$, p^1, q^1, v^1, w^1, as stated in the following proposition.

Proposition 1 *The discrete ECL can be written as*

$$\begin{aligned}
&\frac{1}{2}b^{\mathrm{T}}\Big[\operatorname{diag}(w^1)w^1+\operatorname{diag}(v^1)v^1+2\operatorname{diag}(\theta(ch))\left((p^1)^2+(q^1)^2\right)\\
&+\beta\left((p^1)^2+(q^1)^2\right)^2\Big]h-\tilde{b}^{\mathrm{T}}\left[\operatorname{diag}(v_1)(\partial_t p)_1+\operatorname{diag}(w_1)(\partial_t q)_1\right]\tau\\
=&\frac{1}{2}b^{\mathrm{T}}\Big[\operatorname{diag}(w^0)w^0+\operatorname{diag}(v^0)v^0+2\operatorname{diag}(\theta(ch))\left((p^0)^2+(q^0)^2\right)\\
&+\beta\left((p^0)^2+(q^0)^2\right)^2\Big]h-\tilde{b}^{\mathrm{T}}\left[\operatorname{diag}(v_0)(\partial_t p)_0+\operatorname{diag}(w_0)(\partial_t q)_0\right]\tau,
\end{aligned}\tag{3.6}$$

Thus, the nonlinear system (3.5) can be rewritten as

$$\begin{cases}L(h,\tau,\alpha)Y-F(Y,h)=Y_0,\\ T\left(v_1,w_1,(\partial_t p)_1,(\partial_t q)_1,p^1,q^1,v^1,w^1\right)=T\left(v_0,w_0,(\partial_t p)_0,(\partial_t q)_0,p^0,q^0,v^0,w^0\right),\end{cases}$$

where $Y_0=((p_0\otimes e_s)^{\mathrm{T}},(q_0\otimes e_s)^{\mathrm{T}},(v_0\otimes e_s)^{\mathrm{T}},(w_0\otimes e_s)^{\mathrm{T}},(e_r\otimes p^0)^{\mathrm{T}},(e_r\otimes q^0)^{\mathrm{T}},0_{rs}^{\mathrm{T}},0_{rs}^{\mathrm{T}})^{\mathrm{T}}$, $Y=(P^{\mathrm{T}},Q^{\mathrm{T}},V^{\mathrm{T}},W^{\mathrm{T}},\partial_t P^{\mathrm{T}},\partial_t Q^{\mathrm{T}},\partial_x V^{\mathrm{T}},\partial_x W^{\mathrm{T}})^{\mathrm{T}}$.

$T(v_1,w_1,(\partial_t p)_1,(\partial_t q)_1,\,p^1,q^1,v^1,w^1)$ denotes the left-hand side of (3.6), and

$$L(h,\tau,\alpha)=\begin{pmatrix}L_{11}&L_{12}&O&O\\O&L_{22}&O&L_{24}\\L_{31}&O&L_{33}&O\\O&O&L_{43}&L_{44}\end{pmatrix},\quad F(Y,h)=\begin{pmatrix}\mathbf{0}\\\mathbf{0}\\\mathbf{0}\\F_4\end{pmatrix},$$

here $L_{12}=L_{24}=-hI_2\otimes[I_r\otimes A(\alpha)]$, $L_{33}=\tau I_2\otimes[\tilde{A}(\alpha)\otimes I_s]$, $L_{44}=\frac{1}{2}L_{11}$,

$$\begin{aligned}
&L_{11}=L_{22}=L_{31}=\begin{pmatrix}I_{rs}&O_{rs}\\O_{rs}&I_{rs}\end{pmatrix},\quad O=\begin{pmatrix}O_{rs}&O_{rs}\\O_{rs}&O_{rs}\end{pmatrix},\quad \mathbf{0}=\begin{pmatrix}0_{rs}\\0_{rs}\end{pmatrix},\\
&L_{43}=\begin{pmatrix}I_{rs}&O_{rs}\\O_{rs}&-I_{rs}\end{pmatrix},\quad F_4=\begin{pmatrix}\left(e_r\otimes\theta(ch)+\beta(P^2+Q^2)\right)Q\\\left(e_r\otimes\theta(ch)+\beta(P^2+Q^2)\right)P\end{pmatrix},
\end{aligned}$$

with $O_{rs}\in\mathbb{R}^{rs\times rs}$ and $0_{rs}\in\mathbb{R}^{rs}$ being the zero matrix and zero vector, respectively.

Let $y_0=\left(v_0,w_0,(\partial_t p)_0,(\partial_t q)_0,p^0,q^0,v^0,w^0\right)^{\mathrm{T}}$, $y_1=\left(v_1,w_1,(\partial_t p)_1,(\partial_t q)_1,p^1,q^1,v^1,w^1\right)^{\mathrm{T}}$, and define the error function of the discrete ECL as $G(\alpha)=T(y_1)-T(y_0)$. Next, we use the multi-symplectic RK scheme (2.5) to establish the mapping between y_0 and y_1. From (2.5), we have

$$\begin{aligned}
&p^1_{[i]}=p^0_{[i]}+\tau\sum_{m=1}^{r}\tilde{b}_m\partial_t P_{i,m},\quad v_1^{[m]}=v_0^{[m]}+h\sum_{i=1}^{s}b_i\partial_x V_{i,m},\\
&q^1_{[i]}=q^0_{[i]}+\tau\sum_{m=1}^{r}\tilde{b}_m\partial_t Q_{i,m},\quad w_1^{[m]}=w_0^{[m]}+h\sum_{i=1}^{s}b_i\partial_x W_{i,m}.
\end{aligned}$$

We also introduce four auxiliary systems:

$$\begin{aligned}
&V_{i,m}=v^0_{[i]}+\tau\sum_{n=1}^{r}\tilde{a}_{mn}(\alpha)\partial_t V_{i,n},&&v^1_{[i]}=v^0_{[i]}+\tau\sum_{m=1}^{r}\tilde{b}_m\partial_t V_{i,m},\\
&W_{i,m}=w^0_{[i]}+\tau\sum_{n=1}^{r}\tilde{a}_{mn}(\alpha)\partial_t W_{i,n},&&w^1_{[i]}=w^0_{[i]}+\tau\sum_{m=1}^{r}\tilde{b}_m\partial_t W_{i,m},\\
&\partial_t P_{i,m}=(\partial_t p)_0^{[m]}+h\sum_{j=1}^{s}a_{ij}(\alpha)\partial_t V_{j,m},&&(\partial_t p)_1^{[m]}=(\partial_t p)_0^{[m]}+h\sum_{i=1}^{s}b_i\partial_t V_{i,m},\\
&\partial_t Q_{i,m}=(\partial_t q)_0^{[m]}+h\sum_{j=1}^{s}a_{ij}(\alpha)\partial_t W_{j,m},&&(\partial_t q)_1^{[m]}=(\partial_t q)_0^{[m]}+h\sum_{i=1}^{s}b_i\partial_t W_{i,m},
\end{aligned}$$

where $\partial_{xt}P_{i,m} = \partial_t V_{i,m}$, $\partial_{xt}Q_{i,m} = \partial_t W_{i,m}$. Thus the equations for v_1, w_1, $(\partial_t p)_1$, $(\partial_t q)_1$, p^1, q^1, v^1, w^1 can be rewritten as

$$\begin{aligned}
&p^1 = p^0 + \tau(\tilde{b}^{\mathrm{T}} \otimes I_s)\partial_t P, && q^1 = q^0 + \tau(\tilde{b}^{\mathrm{T}} \otimes I_s)\partial_t Q,\\
&v^1 = v^0 + \tau(\tilde{b}^{\mathrm{T}} \otimes I_s)\partial_t V, && w^1 = w^0 + \tau(\tilde{b}^{\mathrm{T}} \otimes I_s)\partial_t W,\\
&v_1 = v_0 + h(I_r \otimes b^{\mathrm{T}})\partial_x V, && w_1 = w_0 + h(I_r \otimes b^{\mathrm{T}})\partial_x W,\\
&(\partial_t p)_1 = (\partial_t p)_0 + h(I_r \otimes b^{\mathrm{T}})\partial_t V, && (\partial_t q)_1 = (\partial_t q)_0 + h(I_r \otimes b^{\mathrm{T}})\partial_t W.
\end{aligned} \tag{3.7}$$

On an arbitrary $h \times \tau$ rectangular domain, (3.5) is equivalent to the nonlinear system in Y and α:

$$\begin{cases} L(h,\tau,\alpha)Y - F(Y,h) = Y_0, \\ G(\alpha) = 0. \end{cases} \tag{3.8}$$

The solvability of this system ensures the energy conservation of the proposed method. we make the following assumptions:

(S1) The function G is analytic in a cube $\mathcal{D} = [-\alpha_0, \alpha_0] \times [-h_0, h_0] \times [-\tau_0, \tau_0]$;
(S2) $G(0, h, \tau) = c_0\tau^d + \mathcal{O}(\tau^{d+1}), \quad c_0 \neq 0,$
$G(\alpha, h, \tau) = c(\alpha)\tau^{d-m} + \mathcal{O}(\tau^{d+1-m}), \quad c(\alpha) \neq 0.$

Following the proof strategies in [12,11], we obtain the following theorem.

Theorem 3.2 *Let assumptions (S1)-(S2) be satisfied, suppose that either $h \leq \tau^2$ and the RK matrix $\tilde{A}$ is nonsingular, or $\tau \leq h^2$ and A is nonsingular. Then the system* (3.8) *has a unique solution (Y^T, α).*

4 Numerical experiments

In this section, we compare the proposed parametric multi-symplectic RK method with the classical one through several numerical examples. The results show excellent energy conservation and mass preservation of the proposed method. We consider the one-dimensional GPE with a periodic potential:

$$\begin{cases} \mathrm{i}u_t = -\dfrac{1}{2}u_{xx} + \cos^2\left(\dfrac{\pi x}{15}\right)u + |u|^2 u, \quad -30 \leq x \leq 30,\ t > 0, \\ u(x,0) = \sin\left(\dfrac{\pi x}{15}\right), \end{cases} \tag{4.1}$$

under periodic boundary conditions. The exact solution for this problem is

$$u(x,t) = \exp\left(-\mathrm{i}t\left(1 + \frac{\pi^2}{450}\right)\right)\sin\left(\frac{\pi x}{15}\right). \tag{4.2}$$

4.1 Numerical method

We solve (4.1) using the parametric multi-symplectic RK method (Example 3.1), with the midpoint rule ($r = 1$) in time and the fourth-order Gauss collocation method ($s = 2$) in space, taking $\tau = 1/150$ and $h = 1$. The procedure is as follows.

On each $h \times \tau$ rectangular element, with $a_{11} = \frac{1}{4}$, $a_{12} = \frac{1}{4} - \frac{\sqrt{3}}{6}$, $a_{21} = \frac{1}{4} + \frac{\sqrt{3}}{6}$, $a_{22} = \frac{1}{4}$, $b_1 = b_2 = \frac{1}{2}$, $c_1 = \frac{1}{2} - \frac{\sqrt{3}}{6}$, $c_2 = \frac{1}{2} + \frac{\sqrt{3}}{6}$, $\tilde{a}_{11} = \frac{1}{2}$, $\tilde{b}_1 = 1$, $\tilde{c}_1 = \frac{1}{2}$, the system takes the following explicit form:

$$\begin{aligned}
P_{1,1} &= p_0^{[1]} + h\left[a_{11}V_{1,1} + (a_{12} - \alpha)V_{2,1}\right], \\
P_{2,1} &= p_0^{[1]} + h\left[(a_{21} + \alpha)V_{1,1} + a_{22}V_{2,1}\right], \\
Q_{1,1} &= q_0^{[1]} + h\left[a_{11}W_{1,1} + (a_{12} - \alpha)W_{2,1}\right], \\
Q_{2,1} &= q_0^{[1]} + h\left[(a_{21} + \alpha)W_{1,1} + a_{22}W_{2,1}\right],
\end{aligned}$$

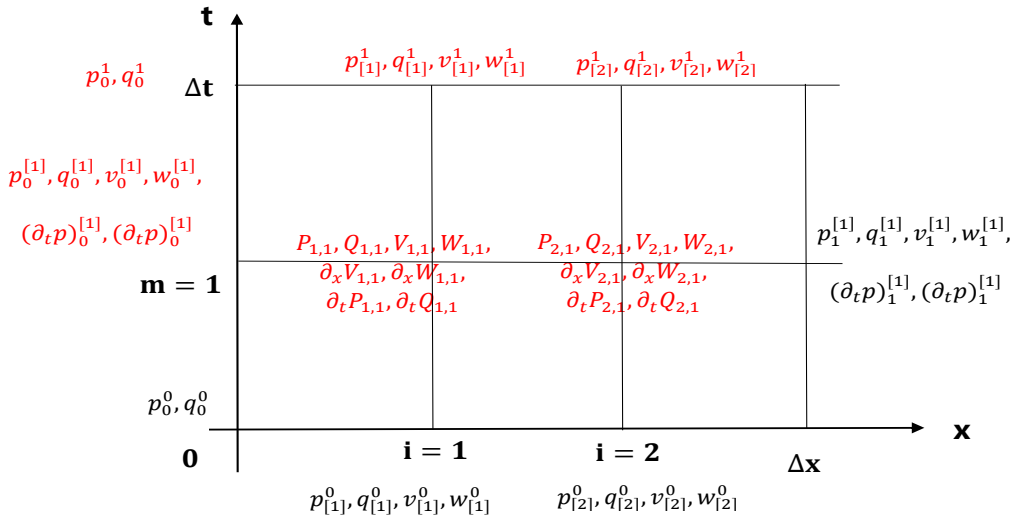


Fig. 4.1: A uniform grid and the unknowns (shown in red) in grid points.

$$
\begin{aligned}
&V_{1,1} = v_0^{[1]} + h\left[a_{11}\partial_x V_{1,1} + (a_{12}-\alpha)\,\partial_x V_{2,1}\right],\\
&V_{2,1} = v_0^{[1]} + h\left[(a_{21}+\alpha)\,\partial_x V_{1,1} + a_{22}\partial_x V_{2,1}\right],\\
&W_{1,1} = w_0^{[1]} + h\left[a_{11}\partial_x W_{1,1} + (a_{12}-\alpha)\,\partial_x W_{2,1}\right],\\
&W_{2,1} = w_0^{[1]} + h\left[(a_{21}+\alpha)\,\partial_x W_{1,1} + a_{22}\partial_x W_{2,1}\right],\\
&p_1^{[1]} = p_0^{[1]} + h(b_1 V_{1,1} + b_2 V_{2,1}),\\
&q_1^{[1]} = q_0^{[1]} + h(b_1 W_{1,1} + b_2 W_{2,1}),\\
&v_1^{[1]} = v_0^{[1]} + h(b_1\partial_x V_{1,1} + b_2\partial_x V_{2,1}),\\
&w_1^{[1]} = w_0^{[1]} + h(b_1\partial_x W_{1,1} + b_2\partial_x W_{2,1}),\\
&P_{1,1} = p_{[1]}^0 + \tau\tilde{a}_{11}\partial_t P_{1,1}, \qquad p_{[1]}^1 = p_{[1]}^0 + \tau\tilde{b}_1\partial_t P_{1,1},\\
&P_{2,1} = p_{[2]}^0 + \tau\tilde{a}_{11}\partial_t P_{2,1}, \qquad p_{[2]}^1 = p_{[2]}^0 + \tau\tilde{b}_1\partial_t P_{2,1},\\
&Q_{1,1} = q_{[1]}^0 + \tau\tilde{a}_{11}\partial_t Q_{1,1}, \qquad q_{[1]}^1 = q_{[1]}^0 + \tau\tilde{b}_1\partial_t Q_{1,1},\\
&Q_{2,1} = q_{[2]}^0 + \tau\tilde{a}_{11}\partial_t Q_{2,1}, \qquad q_{[2]}^1 = q_{[2]}^0 + \tau\tilde{b}_1\partial_t Q_{2,1},\\
&\partial_t P_{1,1} + \frac{1}{2}\partial_x W_{1,1} = \left[\cos^2(c_1 h) + P_{1,1}^2 + Q_{1,1}^2\right] Q_{1,1},\\
&\partial_t P_{2,1} + \frac{1}{2}\partial_x W_{2,1} = \left[\cos^2(c_2 h) + P_{2,1}^2 + Q_{2,1}^2\right] Q_{2,1},\\
&-\partial_t Q_{1,1} + \frac{1}{2}\partial_x V_{1,1} = \left[\cos^2(c_1 h) + P_{1,1}^2 + Q_{1,1}^2\right] P_{1,1},\\
&-\partial_t Q_{2,1} + \frac{1}{2}\partial_x V_{2,1} = \left[\cos^2(c_2 h) + P_{2,1}^2 + Q_{2,1}^2\right] P_{2,1},\\
&h\Big\{\left[b_1(v_{[1]}^1)^2 + b_2(v_{[2]}^1)^2 + b_1(w_{[1]}^1)^2 + b_2(w_{[2]}^1)^2\right]\\
&\quad - \left[b_1(v_{[1]}^0)^2 + b_2(v_{[2]}^0)^2 + b_1(w_{[1]}^0)^2 + b_2(w_{[2]}^0)^2\right]\\
&\quad + \left[b_1\left((p_{[1]}^1)^2 + (q_{[1]}^1)^2\right)^2 + b_2\left((p_{[2]}^1)^2 + (q_{[2]}^1)^2\right)^2\right]\\
&\quad - \left[b_1\left((p_{[1]}^0)^2 + (q_{[1]}^0)^2\right)^2 + b_2\left((p_{[2]}^0)^2 + (q_{[2]}^0)^2\right)^2\right]\\
&\quad + b_1\cos^2(c_1 h)\left[(p_{[1]}^1)^2 + (q_{[1]}^1)^2 - (p_{[1]}^0)^2 - (q_{[1]}^0)^2\right]\\
&\quad + b_2\cos^2(c_2 h)\left[(p_{[2]}^1)^2 + (q_{[2]}^1)^2 - (p_{[2]}^0)^2 - (q_{[2]}^0)^2\right]\Big\}\\
&\quad - \tau\tilde{b}_1\left(v_1^{[1]}(\partial_t p)_1^{[1]} + w_1^{[1]}(\partial_t q)_1^{[1]} - v_0^{[1]}(\partial_t p)_0^{[1]} - w_0^{[1]}(\partial_t q)_0^{[1]}\right) = 0,
\end{aligned}
\tag{4.3}
$$

which has 31 unknowns $P_{1,1}$, $P_{2,1}$, $Q_{1,1}$, $Q_{2,1}$, $V_{1,1}$, $V_{2,1}$, $W_{1,1}$, $W_{2,1}$, $\partial_x V_{1,1}$, $\partial_x V_{2,1}$, $\partial_x W_{1,1}$, $\partial_x W_{2,1}$, $\partial_t P_{1,1}$, $\partial_t P_{2,1}$, $\partial_t Q_{1,1}$, $\partial_t Q_{2,1}$, $p_0^{[1]}$, $q_0^{[1]}$, $v_0^{[1]}$, $w_0^{[1]}$, $p_{[1]}^1$, $p_{[2]}^1$, $q_{[1]}^1$, $q_{[2]}^1$, $v_{[1]}^1$, $v_{[2]}^1$, $w_{[1]}^1$, $w_{[2]}^1$, $(\partial_t p)_0^{[1]}$, $(\partial_t q)_0^{[1]}$ and α. The system (4.3) comprises only 25 equations and requires six supplementary conditions. With $p_0^0 = p(0,0)$ and $q_0^0 = q(0,0)$, we augment (4.3) by the following equations (see [14, Section 3]):

$$\begin{aligned}
p_{[1]}^1 &= p_0^1 + h\left[a_{11} v_{[1]}^1 + (a_{12} - \alpha)\, v_{[2]}^1\right], \\
p_{[2]}^1 &= p_0^1 + h\left[(a_{21} + \alpha)\, v_{[1]}^1 + a_{22} v_{[2]}^1\right], \\
q_{[1]}^1 &= q_0^1 + h\left[a_{11} w_{[1]}^1 + (a_{12} - \alpha)\, w_{[2]}^1\right], \\
q_{[2]}^1 &= q_0^1 + h\left[(a_{21} + \alpha)\, w_{[1]}^1 + a_{22} w_{[2]}^1\right], \\
p_0^{[1]} &= p_0^0 + \tau \tilde{b}_1 (\partial_t p)_0^{[1]}, \qquad p_0^1 = p_0^0 + \tau (\partial_t p)_0^{[1]}, \\
q_0^{[1]} &= q_0^0 + \tau \tilde{b}_1 (\partial_t q)_0^{[1]}, \qquad q_0^1 = q_0^0 + \tau (\partial_t q)_0^{[1]},
\end{aligned} \tag{4.4}$$

where $p_0^1 \approx p(0,\tau)$, $q_0^1 \approx q(0,\tau)$ are unknowns. The resulting nonlinear system (4.3)–(4.4) contains 33 unknowns (see Fig. 4.1).

At each time step, the individual systems are assembled along the spatial direction with $M = 60$ grid points under periodic boundary conditions, yielding a nonlinear system with 1980 unknowns. This system is solved by Newton's method with a convergence tolerance of $\epsilon = 10^{-11}$.

Table 4.1: Temporal convergence rate of the MSRK method with $h = \frac{60}{200}$.

τ	$\frac{1}{4}$	$\frac{1}{8}$	$\frac{1}{16}$	$\frac{1}{32}$
$\|\Im(e^n)\|_{L^2}$	5.02×10^{-2}	1.28×10^{-2}	3.22×10^{-3}	8.17×10^{-4}
order	–	1.97	1.99	2.00
$\|\Im(e^n)\|_{\infty}$	1.07×10^{-2}	2.73×10^{-3}	6.86×10^{-4}	1.74×10^{-4}
order	–	1.97	1.99	1.98

Table 4.2: Spatial convergence rate of the MSRK method with $\tau = \frac{1}{100}$.

h	$\frac{60}{130}$	$\frac{60}{150}$	$\frac{60}{170}$	$\frac{60}{190}$
$\|\Im(e^n)\|_{L^2}$	1.35×10^{-3}	7.04×10^{-4}	3.88×10^{-4}	2.41×10^{-4}
order	–	4.54	4.76	4.27
$\|\Im(e^n)\|_{\infty}$	2.49×10^{-4}	1.31×10^{-4}	7.35×10^{-5}	4.67×10^{-5}
order	–	4.47	4.63	4.08

4.2 **Numerical results**

To verify the convergence order, we employ the following formula

$$\text{order} = \frac{\ln(\|e(s_1)\|_p / \|e(s_2)\|_p)}{\ln(s_1/s_2)},$$

where $e_j^n(s_l) = u(x_j, t_n) - u_j^n$ for $l = 1, 2$ is the error under step size s_l, and the expression $\|\mathbf{e}(s_l)\|_p$ represents the p norm of the error $e_j^n(s_l)$. Here u_j^n and $u(x_j, t_n)$ denote the numerical and exact solutions, respectively.

When $\alpha = 0$, the nonlinear system (4.3)–(4.4) reduces to the classical multi-symplectic RK method, denoted by MSRK. We first examine the spatial and temporal convergence of the MSRK method at the terminal time $T = 1$. To compute the temporal convergence order, a relatively small spatial step $h = 60/200$ is adopted together with various time steps τ listed in Table 4.1. Similarly, in Table 4.2, the time step is fixed at $\tau = 1/100$ to evaluate the spatial convergence. The results in Tables 4.1 and 4.2 indicate that the MSRK method achieves fourth-order accuracy in space and second-order accuracy in time.

Next, we compare the errors in total energy and total mass between the MSRK method and the parametric multi-symplectic RK method (denoted by α-MSRK). The computational domain is

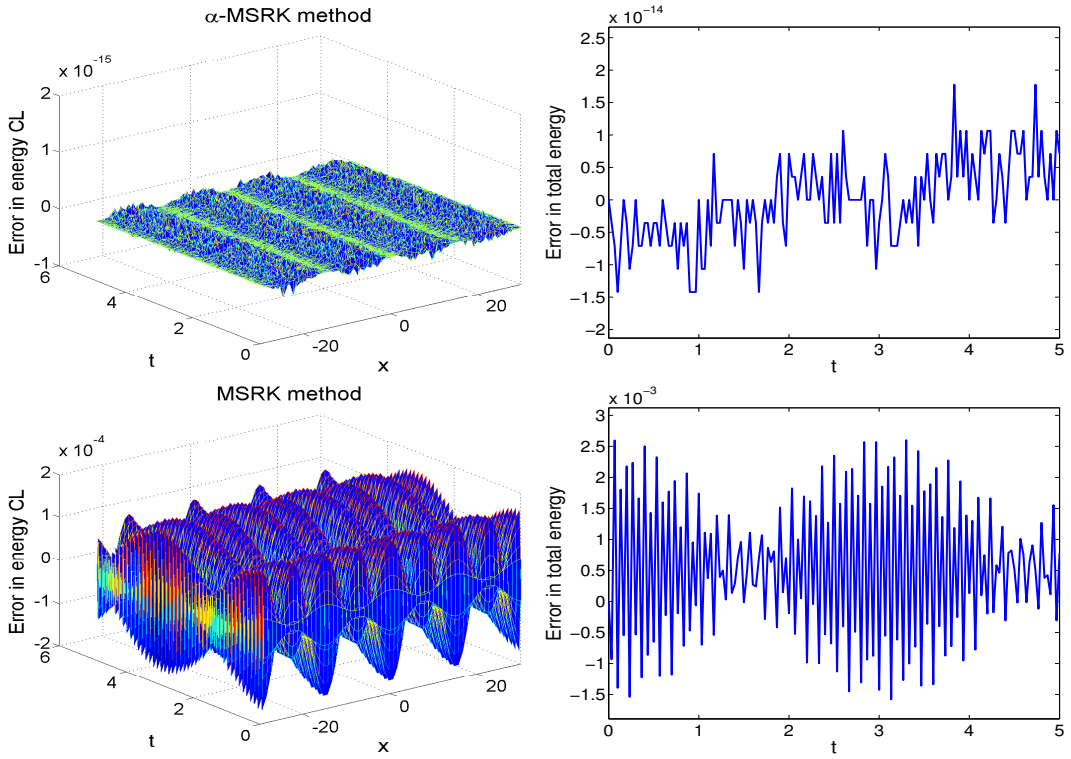


Fig. 4.2: Global and local energy errors of the MSRK and α-MSRK methods on $[0, 5]$.

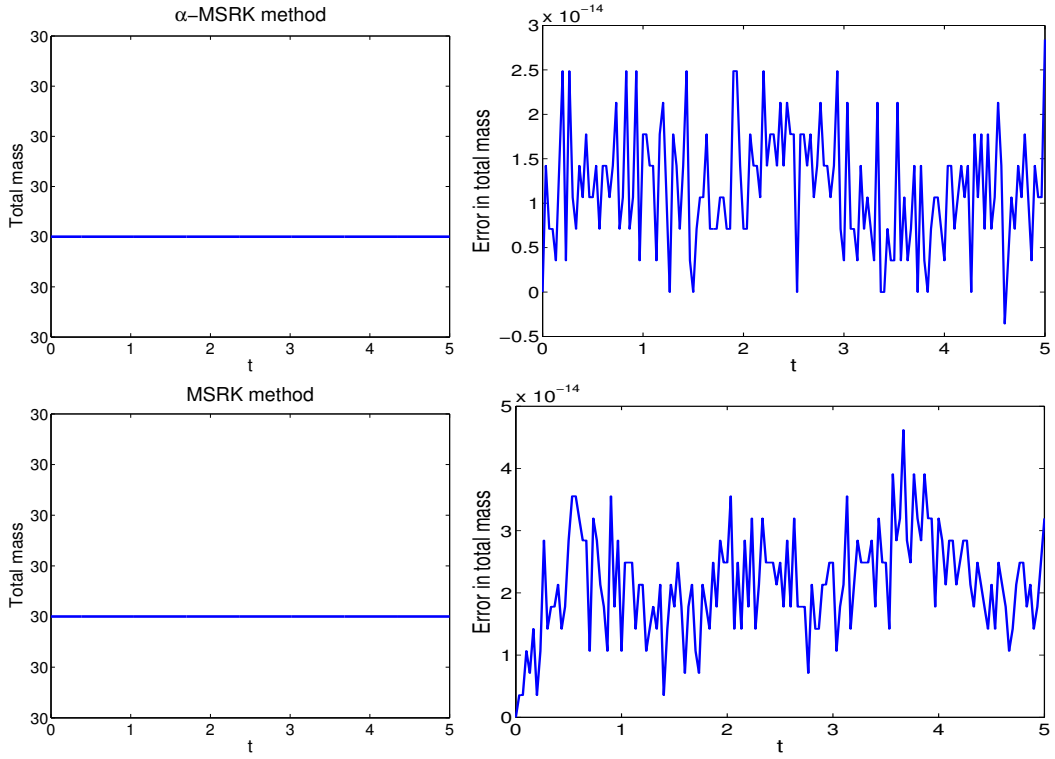


Fig. 4.3: Total mass comparison of the MSRK and α-MSRK methods on $[0, 5]$.

$[-30, 30] \times [0, 5]$ in the (x, t)-plane, with step sizes $h = 1$ and $\tau = 1/150$. The results are shown in Figures 4.2 and 4.3, respectively. For the numerical scheme (4.3)–(4.4), the discrete local mass on each $h \times \tau$ element is defined as

$$\frac{h}{2}\left[\left(p_{[1]}^{n}\right)^{2} + \left(p_{[2]}^{n}\right)^{2} + \left(q_{[1]}^{n}\right)^{2} + \left(q_{[2]}^{n}\right)^{2}\right].$$

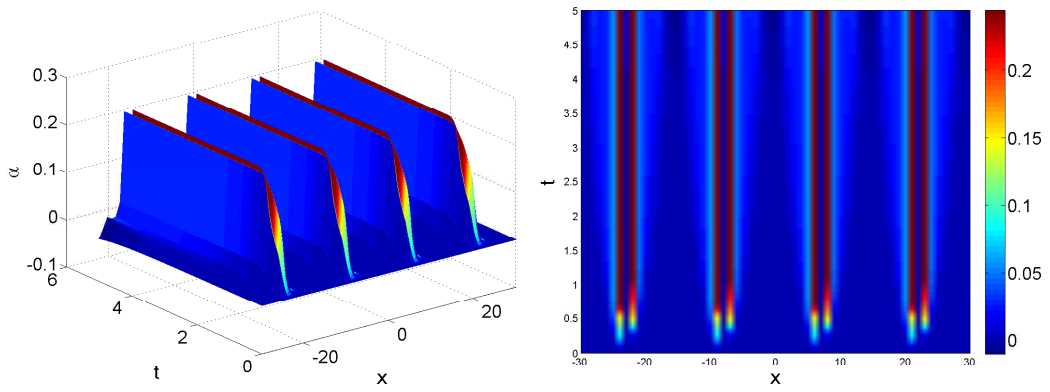


Fig. 4.4: Parameter α distribution of the α-MSRK method on $[-30, 30] \times [0, 5]$ ($h = 1$, $\tau = 1/150$).

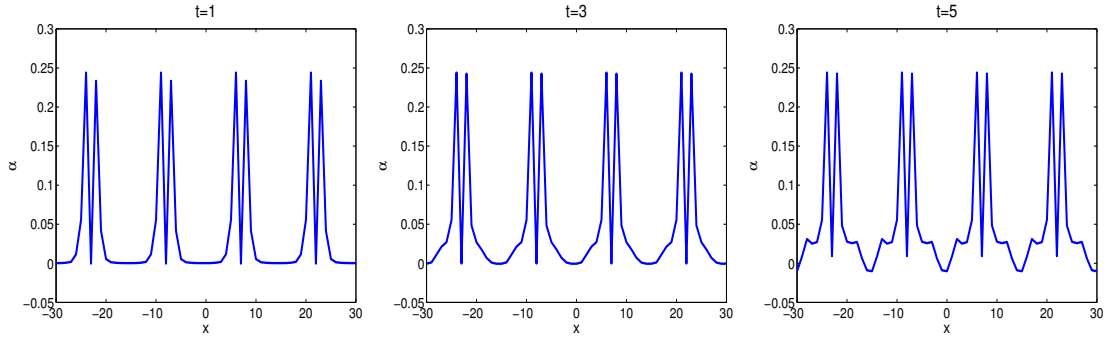


Fig. 4.5: Parameter α of the α-MSRK method on $[-30, 30] \times [0, 5]$ ($h = 1$, $\tau = 1/150$).

That is, we use Gauss quadrature to represent the local mass on each element, rather than directly using $h\big((p_j^n)^2+(q_j^n)^2\big)$. The numerical results show that the α-MSRK method can effectively preserve energy conservation, whereas the MSRK method fails to do so. Furthermore, since the total mass is a quadratic invariant, both the MSRK and α-MSRK methods preserve it exactly.

Figure 4.4 illustrates the values of the parameter α selected by the α-MSRK method for energy conservation on the (x, t)-plane $[-30, 30] \times [0, 5]$. Figure 4.5 provides a detailed profile of the parameter at selected times $t = 1$, $t = 3$, and $t = 5$. The numerical results indicate that such a sequence of parameters exists at every computational grid point.

Figures 4.6–4.8 compare the numerical and exact solutions on $[-30, 30] \times [0, 5]$. The pointwise error distributions at selected times are shown in Figures 4.6 (MSRK) and 4.7 (α-MSRK). The evolution of the exact solution for $t \in [0, 5]$ is displayed in Figure 4.8 for reference. Furthermore, Figure 4.9 compares the phases of the exact and numerical solutions.

5 Conclusions and remarks

The Gross-Pitaevskii equation is a canonical example of Hamiltonian PDEs of the form (2.1), characterized by multiple conservation laws for mass, energy, momentum, and the multi-symplectic structure. We first examine the classical multi-symplectic RK method, which preserves the multi-symplectic structure and quadratic invariants but fails to conserve energy. Motivated by Chen et al. [12], we introduce a parameter α to construct a multi-symplectic perturbation of the classical scheme, termed the EQUIP or parametric multi-symplectic RK method. This perturbed method inherits all conservation properties of the original scheme and additionally achieves energy conservation in a weaker sense, with α depending on the discrete step sizes and initial data. Numerical experiments confirm the expected convergence orders of the classical method and demonstrate the effectiveness of the parametric method in preserving energy and quadratic invariants. Although the higher-dimensional case admits a natural extension, the resulting increase in equations and un-

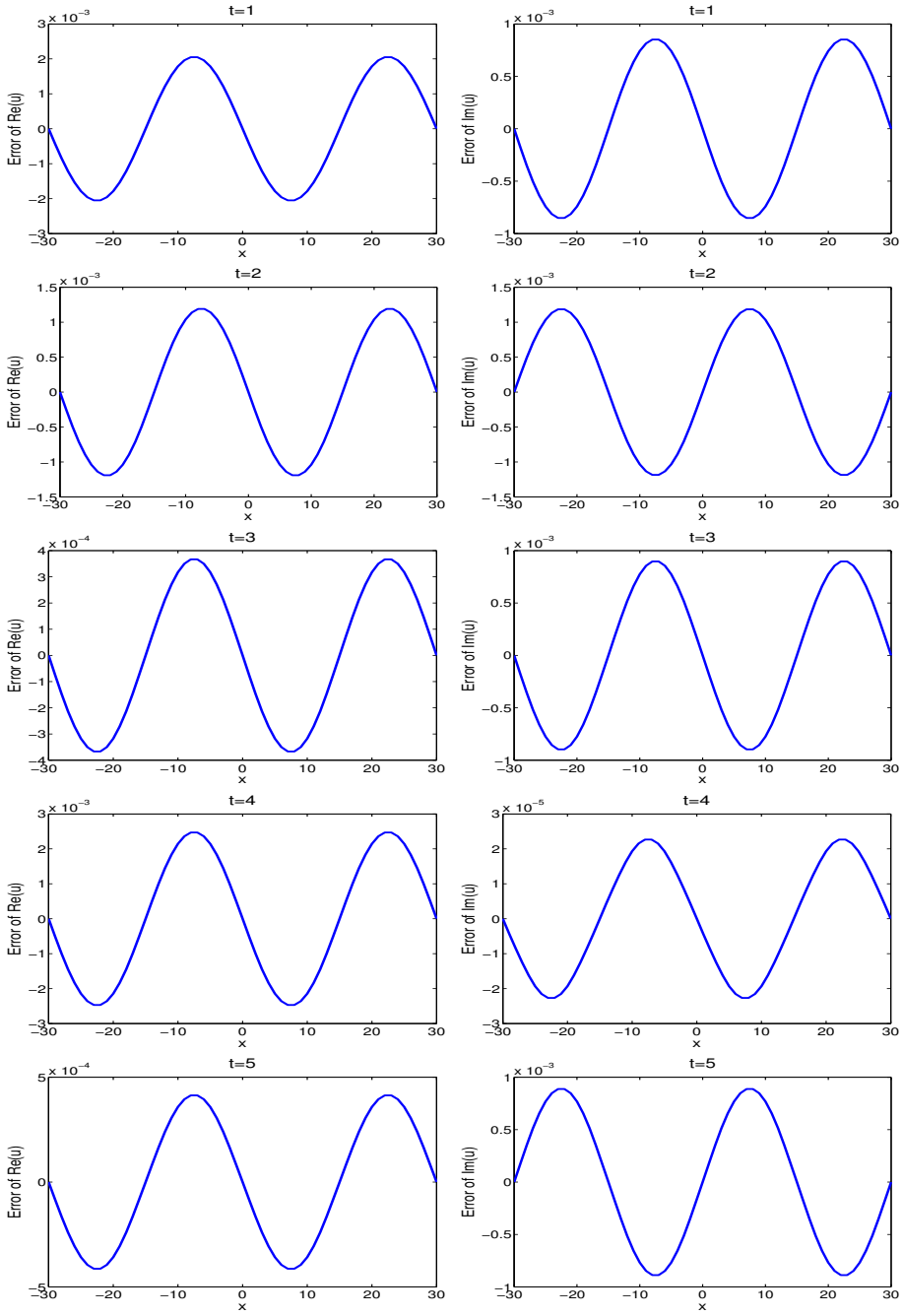


Fig. 4.6: Time evolution of the MSRK error on $[-30, 30] \times [0, 5]$. Left: real part; right: imaginary part.

knowns would substantially degrade computational efficiency. Hence, we restrict our analysis to the one-dimensional setting.

Author Contributions

All authors contributed to writing the manuscript.

Funding

This work was supported by the National Natural Foundation of China (Nos. 12361075, 11961036), Jiangxi Provincial Natural Science Foundation (Nos. 20224ACB201001, 20242BAB25009, 20224BCD41001, 20262BAC240349), China Postdoctoral Science Foundation (No. 2025M773067).

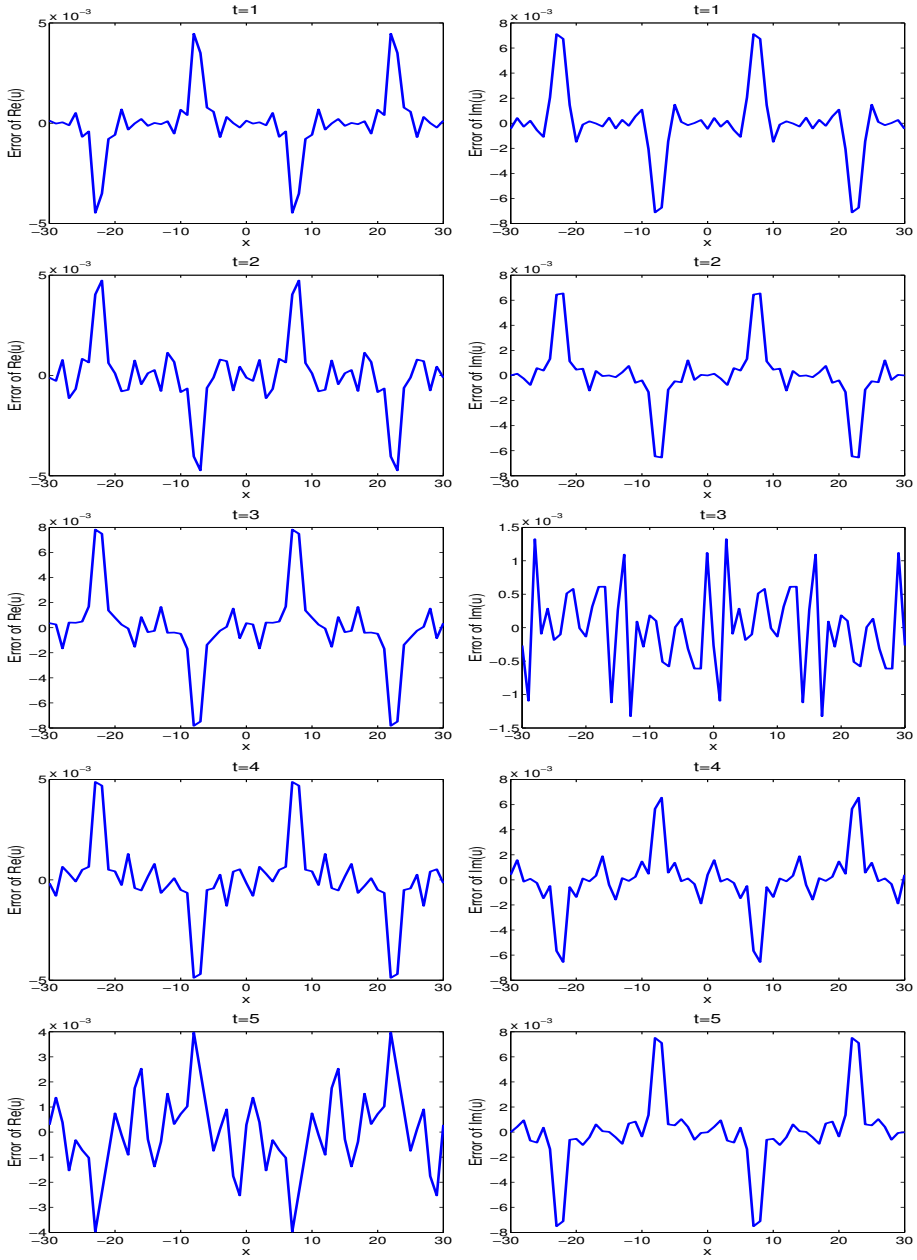


Fig. 4.7: Time evolution of the α-MSRK error on $[-30, 30] \times [0, 5]$. Left: real part; right: imaginary part.

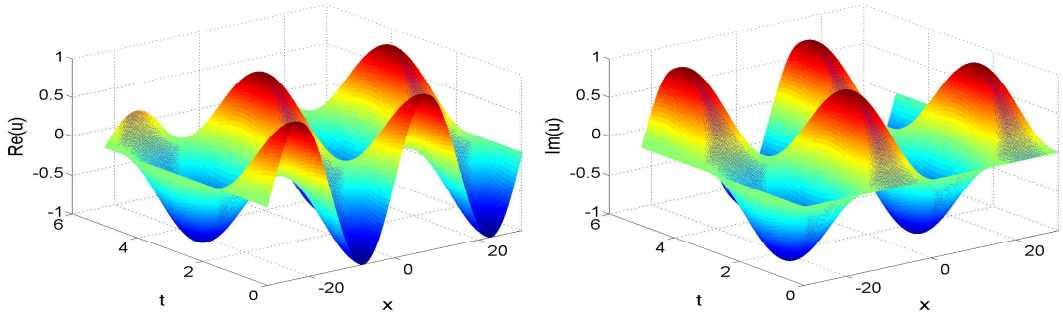


Fig. 4.8: Evolution of the exact solution for $t \in [0, 5]$.

Aknowledgement

We would like to express our sincere gratitude to Professor Jialin Hong and Chuchu Chen at Institute of Computational Mathematics and Scientific/Engineering Computing, Academy of Mathematics

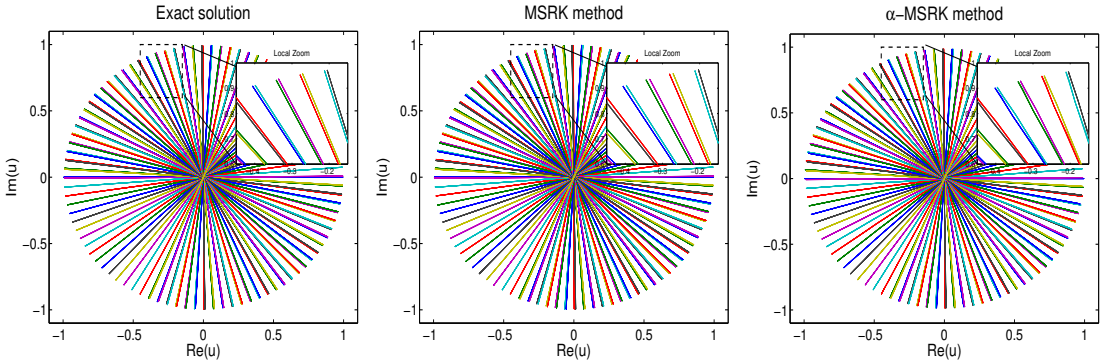


Fig. 4.9: The phase diagram.

and System Science, Chinese Academy of Sciences. They gave invaluable comments to improve the quality of this paper.

Declarations

Conflict of Interest The authors declare no conflict of interest.

References

1. E.P. Gross, Structure of a quantized vortex in boson systems, II Nuovo Cimento Series 10, 20(3): 454-477, 1961.
2. L.P. Pitaevskii, Vortex lines in an imperfect bose gas, Sov. Phys. JETP, 13(2): 451-454, 1961.
3. M.H. Anderson, J.R. Ensher, M.R. Matthews, et al., Observation of Bose-Einstein condensation in a dilute atomic vapor, Science, 269(5221): 198-201, 1995.
4. K.B. Davis, M-O. Mewes, M.R. van Andrews, et al., Bose-Einstein condensation in a gas of sodium atoms, Phys. Rev. Lett., 75(22): 3969-3973, 1995.
5. C.A. Sackett, C.C. Bradley, M. Welling, et al., Bose-Einstein condensation of lithium, Appl. Phys. B, 65(4-5): 433-440, 1997.
6. L. Salasnich, A. Parola, L. Reatto, Effective wave equations for the dynamics of cigar-shaped and disk-shaped Bose condensates, Phys. Rev. A, 65(4): 043614, 2002.
7. A.V. Avdeenkov, K.G. Zloshchastiev, Quantum Bose liquids with logarithmic nonlinearity: Self-sustainability and emergence of spatial extent, J. Phys. B: At. Mol. Opt. Phys., 44(19): 195303, 2011.
8. W. Bao, Y. Cai, Mathematical theory and numerical methods for Bose-Einstein condensation, Kinet. Relat. Mod., 6(1): 1-135, 2013.
9. Y. Gong, C. Jiang, Y. Zhang, Exponential supplementary variable methods for complex-valued Hamiltonian PDEs with applications to rotating Gross-Pitaevskii equation, J. Comput. Phys., 527: 114402, 2025.
10. Z. Ge, J.E. Marsden, Lie-Poisson Hamilton-Jacobi theory and Lie-Poisson integrators, Phys. Lett. A, 133(3): 134-139, 1988.
11. L. Brugnano, F. Iavernaro, D. Trigiante, Energy- and quadratic invariants-preser- ving integrators based upon Gauss collocation formulae, SIAM J. Numer. Anal., 50(6): 2897-2916, 2012.
12. C. Chen, J. Hong, C. Sim, K. Sonwu, Energy and quadratic invariants preserving (EQUIP) multi-symplectic methods for Hamiltonian wave equations, J. Comput. Phys., 418: 109599, 2020.
13. J. Hong, H. Liu, G. Sun, The multi-symplecticity of partitioned Runge-Kutta methods for Hamiltonian PDEs, Math. Comp., 75(253): 167-181, 2006.
14. Y. Wang, J. Hong, Multi-symplectic algorithms for Hamiltonian partial differential equations, Commun. Appl. Math. Comput., 27(2): 163-230, 2013.
15. W. Hu, Z. Deng, S. Han, et al., Generalized multi-symplectic integrators for a class of Hamiltonian nonlinear wave PDEs, J. Comput. Phys., 235: 394-406, 2013.
16. Y. Gong, J. Cai, and Y. Wang, Some new structure-preserving algorithms for general multi-symplectic formulations of Hamiltonian PDEs, J. Comput. Phys., 279: 80-102, 2014.
17. L. Kong, J. Hong and J. Zhang, Splitting multisymplectic integrators for Maxwell's equation, J. Comput. Phys., 229(11): 4259-4278, 2010.
18. S. Reich, Multi-symplectic Runge-Kutta collocation methods for Hamiltonian wave equation, J. Comput. Phys., 157(2): 473-499, 2000.
19. Y. Tian, M. Qin, Y. Zhang, et al., The multisymplectic numerical method for Gross-Pitaevskii equation, Comput. Phys. Commun., 178(6):449-458, 2008.
20. L. Kong, J. Hong, and J. Zhang, LOD-MS for Gross-Pitaevskii equation in Bose-Einstein condensates, Commun. Comput. Phys., 14(1): 219-241, 2013.
21. F. Fu, L. Kong, L. Wang, et al., High order compact splitting multisymplectic schemes for 1D Gross-Pitaevskii equation, Chin. J. Comput. Phys., 35(6): 657-667, 2018.

22. L. Wang, Y. Wang, Multisymplectic structure-preserving scheme for the coupled Gross-Pitaevskii equations, Int. J. Comput. Math., 98(4): 783-806, 2021.
23. J.C. Simo, N. Tarnow, K.K. Wong, Exact energy-momentum conserving algorithms and symplectic schemes for nonlinear dynamics, Comput. Methods Appl. Mech. Engrg., 100(1): 63-116, 1992.
24. D. Wang, A. Xiao, X. Li, Parametric symplectic partitioned Runge-Kutta methods with energy-preserving properties for Hamiltonian systems, Comput. Phys. Commun. 184(2): 303-310, 2013.
25. L. Brugnano, G. Gurioli, F. Iavernaro, Analysis of energy and quadratic invariant preserving (EQUIP) methods, J. Comput. Appl. Math., 335: 51-73, 2018.
26. C. Sim, N. Yun, K. Sonwu, A generalized energy and quadratic invariant preserving (GEQUIP) method for Hamiltonian systems with multiple invariants, J. Comput. Appl. Math., 451: 116084, 2024.
27. J. Cai, Y. Wang, Local energy-preserving scalar auxiliary variable approaches for general multi-symplectic Hamiltonian PDEs, J. Comput. Phys., 521: 113573, 2025.
28. E. Hairer and G. Wanner, Solving Ordinary Differential Equations II. Stiff and DifferentialAlgebraic Problems, 2nd ed., Springer Ser. Comput. Math. 14, Springer, Berlin, 1996.